



ELSEVIER

Contents lists available at ScienceDirect

## Ad Hoc Networks

journal homepage: [www.elsevier.com/locate/adhoc](http://www.elsevier.com/locate/adhoc)

## Combining stochastic geometry and statistical mechanics for the analysis and design of mesh networks

Sunil Srinivasa\*, Martin Haenggi

Emerging Wireless Architectures Laboratory, University of Notre Dame, Notre Dame, IN 46556, United States

### ARTICLE INFO

#### Article history:

Available online xxxxx

#### Keywords:

Multihop networks  
Throughput  
End-to-end delay  
Interference

### ABSTRACT

We consider a two-dimensional mesh network comprising several source-destination pairs, each communicating wirelessly in a multihop fashion. First, we introduce a novel transmission policy for multihop networks according to which all the buffering in the network is performed at source nodes while relays just have unit-sized buffers. We demonstrate that incorporating this buffering scheme in conjunction with minor amendments to the medium access control (MAC) layer yields several benefits such as keeping packet delays small and helping regulate the traffic flow in a completely distributed fashion. Second, we employ a novel combination of tools from stochastic geometry and statistical mechanics to characterize the throughput and end-to-end delay performances of multihop wireless networks for two different channel access mechanisms, Carrier Sense Multiple Access (CSMA) and ALOHA. Our study also offers valuable insights from a system design stand-point such as determining the optimum density of transmitters or the optimal number of hops along a flow that maximizes the system's throughput performance. We corroborate our theoretical analyses via simulations.

© 2011 Elsevier B.V. All rights reserved.

### 1. Introduction

A mesh network is typically formed by randomly deploying nodes that possess self-organizing capabilities and generally consists of several source-destination pairs communicating wirelessly with each other in a decentralized fashion. Multihop routing, where relays assist in the delivery of packets from the sources to the destinations, is the preferred communication strategy in these networks since it helps conserve battery life and efficiently deliver packets over nodes that are far apart. Mesh networks are extremely desirable for several reasons such as being easily and rapidly deployable and reconfigurable, and also for the fact that they lack single points of failure compared to traditional network architectures with infrastructure. However, inherent technical difficulties have stunted the progress from the era of tetherless connectivity predomi-

nated by centralized networks such as cellular telephony and wireless local area networks (WLANs) to the era of ubiquitous wireless connectivity predominated by decentralized mesh networks [1]. We describe the main roadblocks in this regard.

First, while classical information theory has been extremely successful for studying point-to-multipoint links, it is not yet developed enough to characterize the intricacies of multipoint-to-multipoint networks that arise due to the inherent interactions between nodes. In fact, the capacity of a general relay channel with just three nodes is still an open problem. Second, due to the multihop nature of data communication in a mesh network, the flows across various links are spatially and temporally correlated, which needs to be explicitly considered during their analysis and design. Queueing theory has proven useful in this regard, but the analysis gets very cumbersome as the network size grows. Third, in order to optimize the performance of mesh networks, a cross-layer design approach needs to be adopted wherein the interdependencies

\* Corresponding author.

E-mail address: [ssriniv1@nd.edu](mailto:ssriniv1@nd.edu) (S. Srinivasa).

among the layers of the protocol stack, in particular the routing and medium access control (MAC) layers, must be taken into account [2]. Furthermore, the design needs to be adaptive to changes in the system. Owing to such barriers, the performance of general mesh networks has not yet been quantified (beyond scaling laws), and optimal ways of designing and operating them are known only for a few specific and/or simple cases.

In view of these difficulties, researchers are turning to other branches of study to obtain ideas and methodologies that help better understand and characterize the dynamical behavior of wireless networks. Of late, statistical physics has, in particular, captured the attention of the research community since it contains a rich collection of mathematical tools and methodologies for studying interacting many-particle systems. Statistical physics methodologies such as the mean field theory have been employed to study coding over multiuser multiple-input multiple-output (MIMO) channels [3,4]. In [5], the authors have used ideas such as the replica method to characterize the performance of multiuser detection in Code Division Multiple Access (CDMA). The statistical mechanics of interfering transmissions in wireless networks has been proposed in [6,7]. Tools from statistical physics have also been successfully applied to study interesting problems in random communication networks such as percolation, connectivity and capacity [8].

Along similar lines, we employ a novel combination of two new analytical tools, *stochastic geometry* [9] and the *totally asymmetric simple exclusion process* (TASEP) [10], a model in statistical mechanics, to study and design interference-limited wireless networks. Our contributions are twofold:

1. We propose a novel transmission for multihop networks according to which all the buffering is performed at the source nodes while relay nodes have buffer sizes of unity. We demonstrate via simulations that this scheme keeps packet delays small and helps regulate traffic in a completely distributed fashion.
2. We characterize the throughput and end-to-end delay performance of the network for two different channel access schemes using results from stochastic geometry and the TASEP literature. We also provide some insights on optimizing the *throughput density* (to be defined later) in multihop wireless networks that are useful from a design stand-point. Additionally, we validate our analysis with simulations.

To the best of our knowledge, this is the first attempt at combining ideas from stochastic geometry and statistical mechanics.

## 2. System model

### 2.1. Network geometry

We consider a mesh network comprising an infinite number of source nodes, each of which initiates a (in general, multihop) flow of packets to a certain (destination)

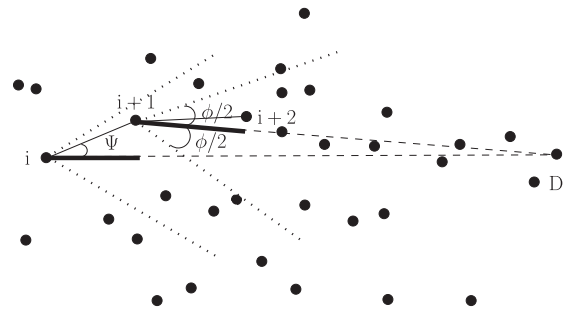


**Fig. 1.** Illustration of nearest-neighbor routing in a sector of angle  $\pm\phi/2$  along the axis to the destination for an arbitrary flow. The packet is routed from node  $i$  to node  $i+1$ , which then relays it to node  $i+2$ . We denote the argument to the destination by the random variable  $\Psi$ . The thick solid lines along the axes to the destination represent the *progress* (to be defined later) of packets across the links  $i \rightarrow i+1$  and  $i+1 \rightarrow i+2$ .

node lasting over an infinite duration of time. This framework is suitable for modeling mesh networks since the aggregate traffic in a mesh network can always be decomposed into several multihop flows. The distribution of source nodes is assumed to be a homogeneous Poisson point process (PPP) on the infinite plane  $\mathbb{R}^2$  with density  $\delta$ . Additionally, the network consists of a countably infinite population of other nodes (potential relays and destinations) arranged as a homogeneous PPP with density  $1 - \delta$ . Thus, the total density of the network is (without loss of generality) equal to unity. For each source node, the destination node is chosen at a random direction, and at a finite distance.

### 2.2. Routing strategy

We take that packets are then routed in a general manner as follows.<sup>1</sup> Each node that receives a packet relays it to its  $n^{\text{th}}$ -nearest neighbor ( $n \geq 1$ ) in a sector of angle  $\phi \in [0, \pi]$ , i.e., the next-hop node is the  $n^{\text{th}}$ -nearest neighbor that lies within  $\pm\phi/2$  of the axis to the destination. Fig. 1 illustrates the case of nearest-neighbor routing ( $n = 1$ ).

A sample realization of the system model comprising several source-destination pairs is shown in Fig. 2 with  $\delta = 0.05$  and  $\phi = \pi/2$ . In the figure, each destination node is taken to be located five nearest-neighbor ( $n = 1$ ) hops away from its corresponding source, at a random direction.

Note that in this setup, the same common relay node may be a part of multiple flows, in particular when  $\delta$  is not small.

### 2.3. Channel model

We consider the case where all nodes use the same frequency band such that simultaneous transmissions cause interference between links. Furthermore, we assume that the transmit power at each transmitting node is equal to unity. Also, we model the attenuation in each link as the product of a large-scale path loss with exponent  $\gamma$  and a

<sup>1</sup> For implementation, each source needs to know its own location and the direction towards its intended destination.

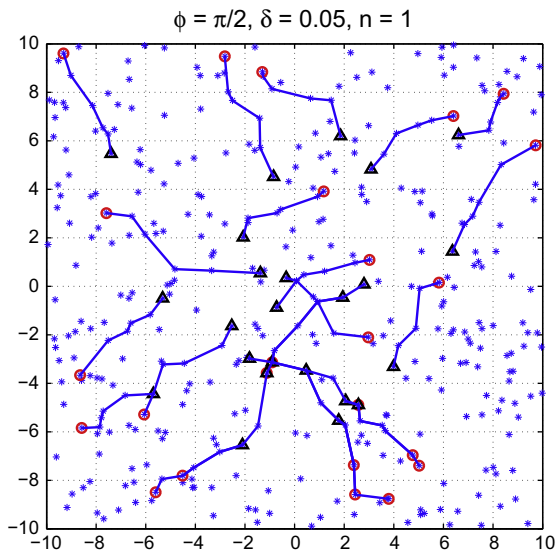


**Fig. 2.** A sample realization of the system model with  $\delta = 0.05$  and  $\phi = \pi/2$ . The triangles depict the sources, while the circles represent destinations. The thick solid lines mark the flows in the network. In this illustration, each destination is assumed to be located five nearest-neighbor ( $n = 1$ ) hops away from its corresponding source node, along a randomly chosen direction.

block i.i.d. Rayleigh fading component. Now, let  $\Phi = \{x_i\}$  denote the set of transmitters in an arbitrary time slot. Then, the total received power at location  $y$  on the plane is

$$I_\Phi(y) = \sum_{x \in \Phi} G_{xy} g(x - y),$$

where  $G_{xy}$  denotes the (power) fading gain of the wireless link between  $x$  and  $y$ , and  $g(z) = \|z\|^{-\gamma}$ . We take the noise power to be negligible compared to interference and define the transmission of a packet from a node located at  $x$  to another located at  $y$  to be successful if and only if the instantaneous signal-to-interference-ratio (SIR) at  $y$  is greater than a threshold  $\Theta$ , i.e., the probability of a successful transmission across the link  $x \rightarrow y$  (denoted by  $p_s$ ) equals

$$p_s = \Pr\left(\frac{G_{xy}\|x - y\|^{-\gamma}}{I_{\Phi \setminus \{x\}}(y)} > \Theta\right). \quad (1)$$

#### 2.4. MAC schemes

We consider a slotted system and study two MAC schemes for each flow in the system: *Carrier Sense Multiple Access (CSMA)* and *ALOHA*. They operate as follows.

- **CSMA:** In (intra-route) CSMA, in each time slot, only a single node in the flow (amongst all the nodes having a packet) gains the right to access the wireless channel.<sup>2</sup> Equivalently, we may take that the transmitting node is chosen uniformly randomly from the set of all nodes in

<sup>2</sup> It is assumed that nodes in a route can detect each others' transmissions. In CSMA, each node verifies the absence of other traffic before transmitting its packets. Note that we do not consider spatial reuse.

the flow having a packet.

The CSMA MAC protocol may also be interpreted as a variant of TDMA wherein the transmitting node is chosen at random (rather than in an orderly manner).

- **ALOHA:** In ALOHA, in every time slot, each node having a packet independently transmits with some (contention) probability  $q$  or remains idle with probability  $1 - q$ .

#### 2.5. Performance metrics

We are interested in the performance of the mesh network in its *steady state* (as  $t \rightarrow \infty$ ). Specifically, in this work, we focus on two important end-to-end metrics: the (spatial) throughput density and the mean end-to-end delay, each evaluated for a typical flow at steady state.

In the remainder of the paper, we suppose that each source-destination pair in the network is separated by  $N$  hops. Since the distribution of nodes is homogeneous, it is sufficient to simply analyze a “typical” flow in the system. Thus, in the rest of this paper, we focus only on a representative flow occurring across  $N$  relays. Furthermore, we take that the source nodes are backlogged, i.e., they always have packets to transmit.

The metrics of interest are formally defined as follows.

- The throughput of the typical flow,  $T(N)$ , is defined as the average number of packets successfully delivered (to the destination) in unit time. The (spatial) **throughput density**,  $\rho_T(N)$ , is then defined as the mean number of packets successfully delivered (in unit time) per unit surface area. Since the density of destination nodes<sup>3</sup> is  $\delta$ ,  $\rho_T(N) = \delta T(N)$ .
- The **mean end-to-end delay**,  $D(N)$ , is defined as the average number of time slots it takes for the packet at the head of the source node<sup>4</sup> to successfully hop to the destination.

All the results in this paper are obtained by averaging over all possible realizations of the channels and the underlying point processes.

### 3. A novel transmission policy for mesh networks

Despite being decentralized, mesh networks are not just intended to carry small volumes of data in an energy-efficient manner, but may also be used to provide broadband services. However, as reported in [11–13], existing buffering schemes for multihop wireless networks involving large buffer sizes and a drop-tail policy have certain inherent drawbacks such as buffer overflows, excessive queueing delays and scheduling issues resulting in uncoordinated transmissions. Consequently, the end-to-end delay and throughput performance in such systems is disappointing.

<sup>3</sup> For each source node, there exists a corresponding destination node.

<sup>4</sup> Note that we consider only the *in-network* delay (and neglect the queueing delay at the source) since the source nodes are always backlogged.

Motivated thus, we propose the following transmission policy for each flow in the network characterized by the following two rules.

1. All the buffering in the network is performed at the source node, while each relay node has a buffer size of unity (for each flow it is associated with). Thus, all the queueing occurs at the source node, while relay nodes may hold at most one packet (per flow).
2. Transmissions are not accepted by relay nodes if their buffer already contains a packet. Furthermore, packets are retransmitted until they are successfully received.

Rule 1 ensures that nodes have at most one packet in their buffer (corresponding to each flow through them) and is favorable for the following reasons.

- First, keeping buffer sizes small can prevent the mean and the variance of the *in-network* end-to-end delay both from getting excessive. Indeed, when buffer capacities are large, several packets may get stacked up, especially when the link quality is poor, thus transportation

of packets across the links get delayed. Fig. 3 plots the empirical mean and variance of the end-to-end delays for CSMA- and ALOHA-based flows for some values of the relays' buffer capacities (denoted by  $K$ ). In both cases, notice the increase in the mean and the variance of the end-to-end delay with increasing buffer size, in particular, at small values of the link reliability  $p_s$ . Equivalently, the packet delays are much more tightly controlled when the buffer sizes are smaller. Thus, depending on the time a packet spends in its buffer, the source node can judiciously decide whether to drop it (and replace it with a more recent packet).

- Second, employing single-sized buffers can also help lessen estimation errors in networked control systems. This is quite critical in applications such as monitoring physical or environmental conditions, or battlefield surveillance. To this end, consider a process evolving as

$$x[k+1] = Ax[k] + w[k], \quad k \in \mathbb{Z}^+,$$

where  $x[k] \in \mathbb{R}^n$  is the process state and  $w[k]$  is the process noise assumed to be AWGN with covariance  $R_w$ . The process state is observed using a sensor that generates measurements, or observations, of the form

$$y[k] = Cx[k] + v[k], \quad k \geq 0,$$

where  $y[k] \in \mathbb{R}^m$  and the measurement noise  $v[k]$  is also AWGN with a positive definite covariance matrix  $\Sigma_v$ . We assume that the pair  $(A, C)$  is observable. Considering the optimal encoder and decoder designs described in [14], the estimation error covariance at time slot  $k$  becomes

$$\text{Error}[k] = \sum_{m=-1}^k \Pr(t_s(k) = m) f_{k-m}(M(m+1)), \quad (2)$$

where  $f(S) = ASA^T + R_w$  is the *Lyapunov recursion* [14], and  $t_s[k] = m$  denotes the event that  $m \leq k$  packets are received by time slot  $k$ .

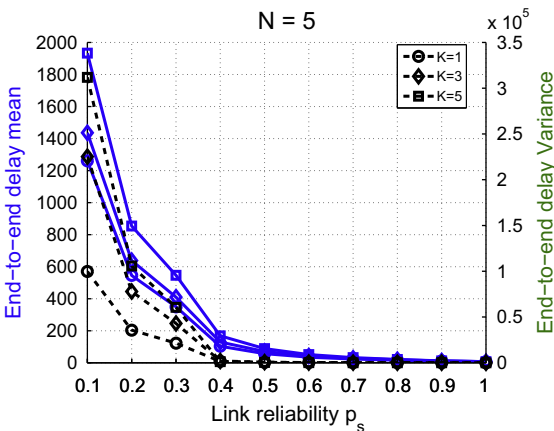
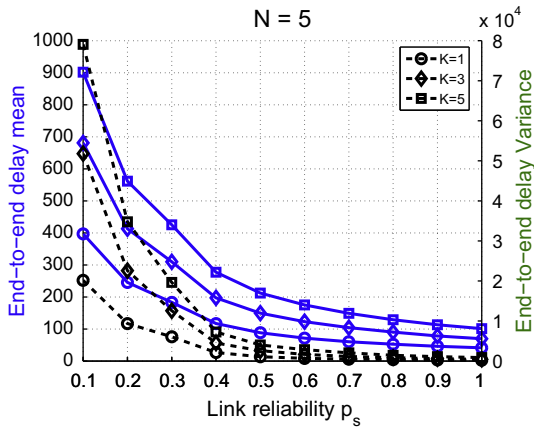


**Fig. 3.** Empirical values of the mean (solid lines) and variance (dashed lines) of the end-to-end delay in CSMA-(top) and ALOHA-based (bottom) wireless flows versus the link reliability and buffer size at nodes. In each case, we see that the larger the buffer capacities of the nodes, the higher are the delay mean and variance.

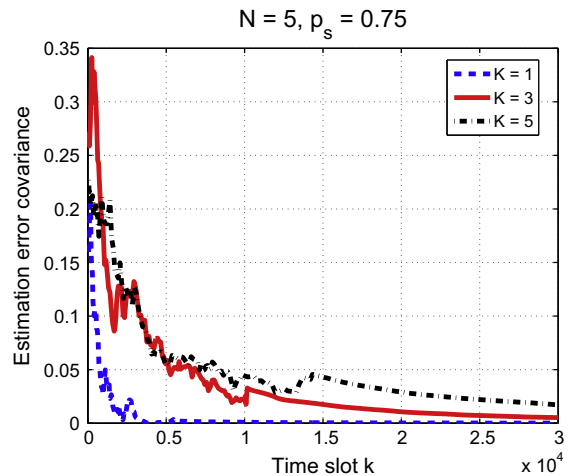


**Fig. 4.** Error Covariance of the estimates for the CSMA-based flow for different values of buffer sizes  $K$ . It is clearly seen that the estimation error converges to its steady state value faster for the single-buffer system.

Fig. 4 plots the time evolution of the error covariance (of the estimated state values) for a CSMA-based flow. We clearly observe that the fastest convergence is obtained for the case  $K = 1$ ; the rate of convergence decreases with increasing buffer size. In essence, the in-network delay for the single-buffer network is the smallest, thus the decoder has access to more observations, and can perform a better estimation of the process states. The same qualitative behavior is expected for the ALOHA-based network as well.

- Third, large buffers increase hardware cost and energy consumption.

Using Rule 1 alone may lead to a loss in throughput due to dropped packets; Rule 2 is needed mainly to reduce interference and consequently keep the number of failed transmissions small. In fact, Rules 1 and 2 together mean that a successful transmission can occur only when a node has a packet to transmit and its target node has an empty buffer. This is a distributed method to prevent packets from getting too closely spaced and ensure spacing between packets in the network, which is essential for the efficient operation of wireless systems that are subject to interference. Together, the rules help efficiently regulate the flow of traffic in the network in a completely distributed fashion. The revised transmission scheme also intrinsically enforces congestion control and works similar to reactive back-pressure algorithms [15] wherein the load at each server is balanced dynamically based on the states of upstream and downstream queues.

## 4. Related work

### 4.1. Review of literature

While wireless networks with single-hop flows are fairly well understood, there has been limited contribution in the study of interference-limited multihop networks. For analytical tractability, previous work on Poisson multihop networks considered only a single link of a typical route (with the implicit assumption that the source-destination distance being infinitely large) and focused on metrics such as energy consumption [16], transmission range [17], spatial density of progress [18,19], or the transmission capacity [20]. Furthermore, prior work assumed that all nodes in the network are backlogged, i.e., they always have packets to transmit. In recent papers [21–23], a problem of similar flavor as the one in this paper was studied, wherein the authors considered a random multihop network and employed tools from basic queueing theory to determine the number of relays and their placements such that the mean network delay is minimized. However, the authors make the idealized assumption that the relays are always located along the source-destination axis, instead of being arranged as a PPP.

In this work, we characterize the performance of mesh networks assuming a more realistic system model than the ones employed earlier. The unified approach used here also has the following advantages. First, it allows for a rigorous and clean analysis. In contrast to prior work, we only consider the nodes that have packets as potential

transmitters. Second, since we consider relays with unit buffer sizes, we only need to concern ourselves with access and retransmission delays, and no queueing analysis (which is often cumbersome) is required. Third, all our results are scalable with respect to the number of hops per route (or equivalently the source-destination separation) and help provide useful insights into the design of wireless networks.

We now provide a brief overview of the one-dimensional TASEP particle flow model. We will see later that each flow in the system model is analogous to the TASEP system and subsequently use results from the TASEP literature, in combination with stochastic geometry, for the analysis.

### 4.2. An overview of the one-dimensional TASEP

The TASEP refers to a family of simple stochastic processes used to describe the dynamics of self-driven systems with several interacting particles and is a paradigm for non-equilibrium systems [10]. The classical 1D TASEP model with open boundaries is defined as follows. Consider a system with  $N + 1$  sites, numbered 0 to  $N$ . Site 0 is taken to be the source that injects particles into the system. The model is said to have open boundaries, meaning that particles are injected into the system at the left boundary (site 1) and exit the system on the right boundary (site  $N$ ). The *configuration* of site  $i$ ,  $1 \leq i \leq N$  at time  $t$  is denoted by  $\tau_i[t]$ , which can only take values in  $\{0, 1\}$ , i.e., each site  $1 \leq i \leq N$  may either be *occupied* (denoted as  $\tau_i[t] = 1$ ) or *empty* (denoted as  $\tau_i[t] = 0$ ). The source, however, is taken to be always occupied ( $\tau_0[t] \equiv 1, \forall t > 0$ ).

In the discrete-time version of the TASEP, the movement of particles is defined to occur in time steps. Specifically, let  $(\tau_1[t], \tau_2[t], \dots, \tau_N[t]) \in \{0, 1\}^N$  denote the configuration of the system in time slot  $t$ . In the subsequent time slot  $t + 1$ , a set of sites is chosen at first, depending on the *updating procedure*. Then, for every site picked, if it contains a particle and the neighboring site on its right has none, then the particle hops from that site to its neighbor with a certain probability  $p$ . Formally, supposing that the  $i$ th site is chosen in time slot  $t$ , we have

$$\mathbb{P}(\tau_i[t + 1] = 0) = 1 - \tau_i[t](1 - p + p\tau_{i+1}[t]),$$

$$\mathbb{P}(\tau_i[t + 1] = 1) = \tau_i[t](1 - p + p\tau_{i+1}[t]).$$

and

$$\mathbb{P}(\tau_{i+1}[t + 1] = 0) = (1 - \tau_{i+1}[t])(1 - p\tau_i[t]),$$

$$\mathbb{P}(\tau_{i+1}[t + 1] = 1) = p\tau_i[t] + \tau_{i+1}[t](1 - p\tau_i[t]).$$

This way, the particles are transported from site 0 through the system until their eventual exit at site  $N$ . The movement of particles to the right is equivalent to the movement of *holes* (or empty sites) to the left. This *particle-hole symmetry* leads to some interesting system dynamics, as we shall see later.

In this paper, we focus on the following two commonly considered TASEP updating procedures:

1. *Random-sequential TASEP*: In each time step, a single site is uniformly randomly picked (w.p.  $1/(N + 1)$ ) for transmission, and particle hopping is performed as per the aforementioned rules.

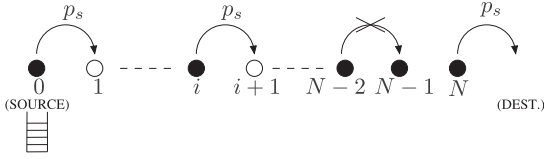


**Fig. 5.** Depiction of a typical flow with the link reliabilities  $p_s$ . The source node (numbered 0) is always backlogged and has a large buffer that feeds packets required to be delivered. Relays  $1, \dots, N$  have buffer sizes of unity. In the above figure, filled circled represent nodes with packets while empty circles indicate nodes with empty buffers. For this snapshot, we see that a transmission from node  $N - 2$  to node  $N - 1$  will fail because  $\tau_{N-1} = 1$ .

2. *Parallel TASEP*: The updating rules are simultaneously applied to all the sites, i.e., in each time slot, all particles having an empty site to their right may jump concurrently.

For both these updating procedures, it is known that in the long time limit ( $t \rightarrow \infty$ ), the TASEP system attains a steady state wherein the rate of particle flow becomes a constant [10].

It is apparent from the description of the TASEP model that it exhibits a similarity to the flows in the wireless network. The sites can be taken to represent the relay nodes and the particles the packets. The hopping probability  $p$  is analogous to the link reliability  $p_s$  while the exclusion principle models the unit buffer size at the relay nodes. Also, the random sequential and parallel updating procedures in the TASEP model relate to the CSMA and ALOHA MAC schemes respectively. Fig. 5 depicts the TASEP-equivalence of the network flow, wherein we assume that the backlogged source has a large buffer and regulates the packet flow into a TASEP model.

For a typical flow across  $N$  relay nodes, we denote the configuration of node  $i$ 's buffer (corresponding to that flow) in time slot  $t$  by  $\tau_i[t]$ ,  $0 \leq i \leq N$ . We take  $\tau_i[t] = 1$  when node  $i$ 's buffer is occupied, i.e., it has a packet, and  $\tau_i[t] = 0$  otherwise. Since the source node is always backlogged,  $\tau_0[t] = 1$ ,  $\forall t$ . Note that a packet may successfully hop between nodes  $i$  and  $i + 1$  in time slot  $t$  only if  $(T_i[t], T_{i+1}[t]) = (1, 0)$ , and furthermore, if its transmission is successful, which happens with probability (w.p.)  $p_s$ .

## 5. Analysis and design of CSMA-based wireless networks

In this section, we analyze the delay and throughput performance of CSMA-based mesh networks employing ideas from stochastic geometry and the random sequential TASEP literature. Our analysis helps provide some useful insights into system design such as choosing the optimal density of source nodes or the number of hops along a route that maximizes the spatial density of throughput. We begin by presenting the following lemma.

**Lemma 5.1** (Corollary 3, [24]). *In a PPP with density  $\lambda$ , the probability density of the distance  $R_n$  from any node to its  $n$ th-nearest-neighbor in a sector of angle  $\phi$  is*

$$p_{R_n}(r) = r^{2n-1} \left(\frac{\lambda\phi}{2}\right)^n \frac{2}{(n-1)!} e^{-\lambda r^2 \phi/2}, \quad r \in \mathbb{R}^+. \quad (3)$$

Furthermore, we have

$$\mathbb{E}[R_n] = \sqrt{\frac{2}{\lambda\phi}} \frac{\Gamma(n+1/2)}{\Gamma(n)} \approx \sqrt{\frac{2}{\lambda\phi}} \sqrt{n-1 + \frac{\pi}{4}}. \quad (4)$$

The approximation may be obtained by using the series expansion of the  $\Gamma$  function, and is a generalization of [16, Eqn. 19]. For  $n$  large,  $\mathbb{E}[R_n] \approx \sqrt{2n/\lambda\phi}$ .

### 5.1. Packet success probability

We next measure the packet success probabilities defined as the probability of a successful packet transmission. The following proposition evaluates the packet success probability for the transmission across a typical link,<sup>5</sup> i.e., between an arbitrary node and its  $n$ th-nearest-neighbor in the CSMA-based network.

**Proposition 5.2.** *For the CSMA-based mesh network, the probability of a successful transmission  $p_s = \mathbb{P}[\text{SIR} > \Theta]$  from any node to its  $n$ th-nearest-neighbor in a sector  $\phi$  is*

$$p_s = \left(\frac{(1-\delta)\phi}{(1-\delta)\phi + 2\delta c}\right)^n, \quad (5)$$

where  $c = \pi\Gamma(1+2/\gamma)\Gamma(1-2/\gamma)\Theta^{2/\gamma}$ .

**Proof.** Recall that for the CSMA MAC scheme, a randomly chosen node having a packet transmits in each flow. Thus, the set of interferers in any time slot<sup>6</sup> forms a homogeneous PPP with density  $\delta$ . From [18, Corollary 3.2], the success probability  $p_s(r)$  across any link of length  $r$  in a Poisson network equals

$$p_s(r) = e^{-\delta c r^2}, \quad (6)$$

with  $c$  given above.

Given that the relay node density is  $(1-\delta)$ , we may put together (3) (with  $\lambda = 1-\delta$ ) and (6) to obtain the success probability of a packet transmission across  $n$ th-nearest-neighbors as

$$\begin{aligned} p_s &= \left(\frac{(1-\delta)\phi}{2}\right)^n \frac{2 \int_0^\infty e^{-((1-\delta)\phi/2 + \delta c)r^2} r^{2n-1} dr}{(n-1)!} \\ &= \left(\frac{(1-\delta)\phi}{(1-\delta)\phi + 2\delta c}\right)^n \frac{\int_0^\infty e^{-t} t^{n-1} dt}{(n-1)!}, \end{aligned} \quad (7)$$

where the latter equality is obtained by a simple change of variables  $t = ((1-\delta)\phi/2 + \delta c)r^2$ . Noting that the integral evaluates to  $\Gamma(n) = (n-1)!$ , (7) simplifies to (5).  $\square$

### 5.2. Node buffer occupancies

We now use ideas from the random sequential TASEP particle flow model [25] to study the dynamics of packet transport in a typical route (across  $N$  relays) in the system at steady state. We begin by noting that as  $t \gg 0$ , the

<sup>5</sup> Basically, any link along a typical route is said to be a typical link. Since the nodal arrangement is homogeneous, the packet success probability across every typical link in the network is the same.

<sup>6</sup> We neglect the temporal correlation of the interference.

probabilities  $\mathbb{P}(\tau_i[t] = 0)$  (and  $\mathbb{P}(\tau_i[t] = 1)$ ),  $0 \leq i \leq N$ , become temporally stationary (independent of time) [25]. We thus drop the dependence on  $t$ , and define  $\mathbb{P}(\tau_i = 1)$  to be the steady state *occupancy* of node  $i$ . In other words, the occupancy of node  $i$  is the same as the average number of packets at the  $i$ th node's buffer. Now, since  $\tau_i$  can take values only in  $\{0, 1\}$ ,  $\mathbb{P}(\tau_i = 1) = \mathbb{E}\tau_i$  and  $\mathbb{P}(\tau_i = 0) = 1 - \mathbb{E}\tau_i$ . From [25, Eqn. 48], we have for  $0 \leq i \leq N$ ,

$$\mathbb{E}\tau_i = \frac{1}{2} + \frac{1}{4} \frac{(2i)!}{(i!)^2} \frac{(N!)^2}{(2N+1)!} \frac{(2N-2i+2)!}{[(N-i+1)!]^2} (N-2i+1),$$

which, is surprisingly, independent of the link reliability  $p_s$ .

In particular, the values at the end nodes are

$$\mathbb{E}\tau_1 = \frac{3N}{2(2N+1)} \quad \text{and} \quad \mathbb{E}\tau_N = \frac{N+2}{2(2N+1)}. \quad (8)$$

Notice the *particle-hole symmetry*, i.e.,  $\mathbb{E}\tau_i = 1 - \mathbb{E}\tau_{N+1-i}$ . Hence, in a system with an odd number of relays, the middle relay has an occupancy of exactly  $1/2$ . Also, note that the average number of occupied sites is  $\sum_{i=0}^N \mathbb{E}\tau_i = 1 + N/2$ .

### 5.3. Steady state throughput and average end-to-end delay

The following theorem uses the occupancies to characterize the throughput and end-to-end delay for a typical flow in the CSMA-based mesh network.

**Theorem 5.3.** *For an CSMA-based flow across  $N$  relays, the throughput at steady state is*

$$T(N) = \frac{p_s}{2N+1}, \quad (9)$$

while the average end-to-end delay is

$$D(N) = \frac{2N^2 + 5N + 2}{2p_s}, \quad (10)$$

where  $p_s$  is as given in (5).

**Proof.** Consider first that an arbitrary node is picked for transmission with probability  $1/(N+1)$ , as in the random sequential TASEP. At any instant of time, relay node  $N$ 's buffer contains a packet w.p.  $\mathbb{E}\tau_N$ ; furthermore, it is picked for transmission (w.p.  $1/(N+1)$ ), and the transmission is successful w.p.  $p_s$ . Thus, the throughput across the flow is simply

$$T(N) = p_s \mathbb{E}\tau_N / (N+1). \quad (11)$$

Now, instead of picking any of the  $N+1$  nodes randomly, if one only chooses among the nodes having a packet, the throughput is improved by a factor of  $N+1 / (\sum_{i=0}^N \mathbb{E}\tau_i) = 2(N+1)/(N+2)$ , i.e.,

$$T(N) = \frac{2p_s \mathbb{E}\tau_N}{N+2}. \quad (12)$$

Using (8) in (12), we obtain the desired result. Since the reliability of the network is 100%, the rate of packets across each link is the same, and equal to (9).

Recall that at steady state, the average number of packets in the flow is  $\sum_{i=0}^N \mathbb{E}\tau_i = 1 + N/2$ . By Little's theorem [26],  $D = \sum_{i=0}^N \mathbb{E}\tau_i / T$ , which equals (10).  $\square$

Putting together Proposition 5.2 and Theorem 5.3, we obtain the throughput for a  $N$ -hop CSMA-based route wherein routing is performed across  $n$ th-nearest neighbors in a sector  $\phi$  as

$$T(N) = \left( \frac{(1-\delta)\phi}{(1-\delta)\phi + 2\delta c} \right)^n \frac{1}{2N+1}. \quad (13)$$

In Section 8, we verify the correctness of (13) via simulations.

We remark that even though the CSMA scheme dictates only a single transmission per flow, in principle, intra-route spatial reuse can also be incorporated into the model. Indeed, suppose that in each time slot, for every node  $i$  that gains the right to access the channel, several nodes  $\dots$ ,  $i-m, i, i+m, \dots$  are also allowed to transmit, where  $m$  is chosen such that simultaneous transmissions occurring at nodes  $m$  hops apart still does not cause intra-flow interference. While several (approximately  $N/m$ ) nodes harness the same space, the density of interferers from other flows' transmissions also (approximately) increases to  $m\delta$ . Manipulating (13), we see that the throughput across a typical flow becomes<sup>7</sup>

$$\begin{aligned} T(N) &\approx \left( \frac{(1-m\delta)\phi}{(1-m\delta)\phi + 2m\delta c} \right)^n \frac{N}{m(2N+1)} \\ &\sim \left( \frac{(1-m\delta)\phi}{(1-m\delta)\phi + 2m\delta c} \right)^n \frac{1}{2m}. \end{aligned} \quad (14)$$

Depending on the values of  $\delta$  and  $\Theta$ , employing spatial reuse may turn out to be beneficial or not.

We next provide some useful insights from a system design stand-point such as determining the optimal fraction of sources and the optimum number of hops between the source and destination such that the throughput density of the network is maximized. For clarity, we treat the cases  $n=1$  and  $n>1$  separately.

### 5.4. Nearest-neighbor routing

Assume that the source-destination distance can be traversed in  $N+1$  nearest-neighbor hops (or equivalently, across  $N$  relays). For the case  $n=1$ , the throughput density is (using (13))

$$\rho_T(N) = \frac{1}{2N+1} \frac{(1-\delta)\delta\phi}{(1-\delta)\phi + 2\delta c}. \quad (15)$$

Clearly, for small  $\delta$ , the throughput density is small. As  $\delta$  increases, the density of flows increases as well, thus the throughput performance of the network improves. However, as  $\delta$  gets very large, the interference in the network becomes high, and the link reliabilities begin to drop, resulting in a decreased throughput density. Evidently, there exists an optimum value of  $\delta$  that maximizes the throughput density of the network.

<sup>7</sup> For two functions  $f$  and  $g$ , the notation  $f(N) \sim g(N)$  means that the ratio  $f(N)/g(N)$  approaches 1 asymptotically (as  $N \rightarrow \infty$ ).

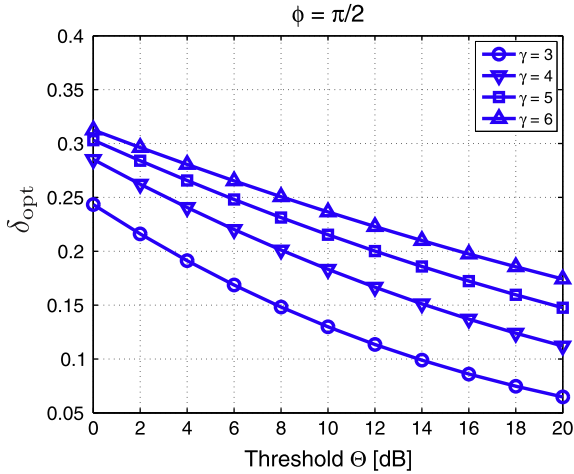


**Fig. 6.** The optimum values of  $\delta$  (16) that maximize the throughput density in the CSMA-based network employing the nearest-neighbor routing strategy for several  $\Theta$  and  $\gamma$  values.

Differentiating (15) w.r.t.  $\delta$  and equating to 0 yields

$$(\phi - 2c)\delta^2 - 2\phi\delta + \phi = 0.$$

Noting that  $0 \leq \delta \leq 1$ , we see that  $\rho_T$  is maximized at

$$\delta_{\text{opt}} = \frac{\phi - \sqrt{2\phi c}}{\phi - 2c}, \quad (16)$$

irrespective of the value of  $N$ .

Fig. 6 plots the throughput density-maximizing values of  $\delta$  versus the threshold  $\Theta$  for the network adopting nearest-neighbor routing and the CSMA MAC scheme for several values of the path loss exponent (PLE)  $\gamma$ . As expected intuitively, the higher the threshold  $\Theta$  and/or smaller the PLE  $\gamma$ , the smaller is the packet success probability  $p_s$ , thus the smaller is the optimum fraction of sources  $\delta_{\text{opt}}$ .

### 5.5. $n$ th-nearest-neighbor Routing ( $n > 1$ )

Supposing now that each relay that receives a packet forwards it to its  $n$ th-nearest neighbors ( $n > 1$ ). For a fair comparison of the routing schemes for different  $n$ , we take the total average progress<sup>8</sup> made by the packet to be the same for every value of  $n$ .

Now, recall that for the case  $n = 1$ , the mean progress<sup>9</sup> of the packet over  $N + 1$  hops is

$$\Delta = (N + 1)\mathbb{E}[R_1 \cos(\Psi)] = (N + 1)\mathbb{E}[R_1]\mathbb{E}[\cos \Psi], \quad (17)$$

where  $\Psi$  is the argument of the destination node (see Fig. 1). Since  $\Psi$  is uniformly distributed on  $[-\phi/2, \phi/2]$ , we have

$$\mathbb{E}[\cos \Psi] = \int_{-\phi/2}^{\phi/2} \frac{1}{\phi} \cos \psi \, d\psi = \frac{2}{\phi} \sin\left(\frac{\phi}{2}\right). \quad (18)$$

<sup>8</sup> The progress of a packet across any link is defined as the effective distance travelled by it along the axis to the destination (see Fig. 1). The total progress is the sum of the progresses across all the links from the source to the destination.

<sup>9</sup> The expectation is taken over several different realizations of the underlying PPP.

Substituting for (4) and (18) in (17), we obtain the average total progress of packets (from the source to the destination) as

$$\Delta = \frac{(N + 1)\sqrt{2\pi} \sin(\phi/2)}{\sqrt{(1 - \delta)\phi^{3/2}}}.$$

For the general case of  $n$ th-nearest-neighbor routing ( $n > 1$ ), the per-hop progress in this case is  $\mathbb{E}[R_n]\mathbb{E}[\cos \Psi]$ . Thus, the number of hops  $N'$  required to achieve the same average (total) progress is approximately

$$N' = (N + 1)\mathbb{E}[R_1]/\mathbb{E}[R_n] \sim N/\sqrt{n}, \quad (19)$$

using (4). Thus, for a flow employing  $n$ th-nearest-neighbor routing, the number of relays in the flow is approximately  $N/\sqrt{n}$ .

The throughput density in the general case then becomes

$$\rho_T(N) = \frac{\delta\sqrt{n}}{2N + \sqrt{n}} \left( \frac{(1 - \delta)\phi}{(1 - \delta)\phi + 2\delta c} \right)^n. \quad (20)$$

Following the same steps as earlier, the throughput density-maximizing (optimal) value of  $\delta$  is obtained as

$$\delta_{\text{opt}} = \frac{(n - 1)c + \phi - \sqrt{(n - 1)^2 c^2 + 2n\phi c}}{(\phi - 2c)}, \quad (21)$$

which is also independent of  $N$ . The values of  $\delta_{\text{opt}}$  versus the routing parameter  $n$  are plotted in Fig. 7 for different values of the PLE  $\gamma$ .

Another critical design issue in wireless networks is determining the optimum routing parameter  $n$ . Indeed, as argued in [27], a smaller hop length does not necessarily relate to an improved network performance. Differentiating (20) with respect to  $n$ , and equating to 0, we obtain

$$\left(2n + \frac{n^{3/2}}{N}\right) \ln\left(1 + \frac{2\delta c}{(1 - \delta)\phi}\right) - 1 = 0. \quad (22)$$

The throughput density-maximizing routing parameter  $n_{\text{opt}}$  may be evaluated analytically. Fig. 8 shows optimum

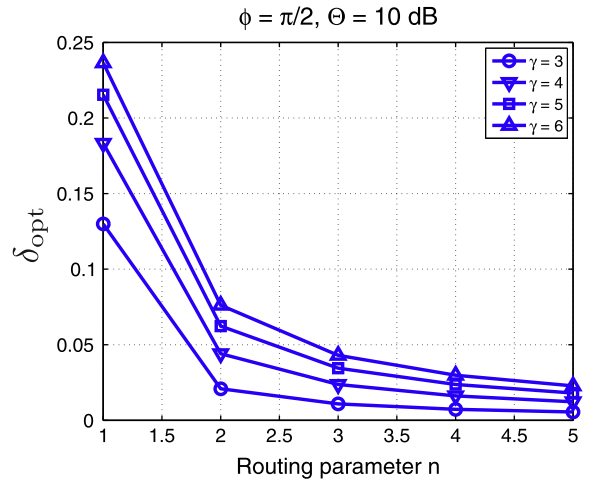


**Fig. 7.** The optimum values of  $\delta$  (21) that maximize the throughput density in the CSMA-based network employing the  $n$ th-nearest-neighbor routing scheme for different values of  $\Theta$  and  $\gamma$ .



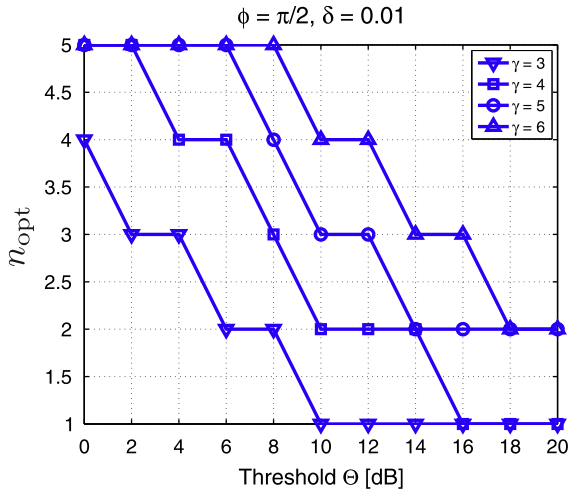


**Fig. 8.** The optimum values of  $n$  (22) that maximize the throughput density in a CSMA-based network with  $N=4$  nodes versus the SIR threshold for successful transmissions,  $\Theta$ .

values of the routing parameter  $n_{\text{opt}}$  (rounded off to the nearest integer) that maximize the throughput density in the network for several values of  $\Theta$  and  $\gamma$ .

## 6. Analysis and design of ALOHA-based wireless networks

In this subsection, we analyze the end-to-end delay and throughput performances of mesh networks with ALOHA. For our analysis, we use known results from the parallel TASEP literature [28].

### 6.1. Node buffer occupancies

First, we study the buffer occupancies for an ALOHA-based flow in the network. Since the nodal arrangement is homogeneous, the reliability across each link the network is the same (and equal to  $p_s$ ). With  $q$  being the ALOHA contention parameter, we may take the “effective” hopping probability in the corresponding parallel TASEP model to be  $p = qp_s$ . Note that in general, the link reliability  $p_s$  is a function of the contention probability  $q$ , since the interference in the network depends on  $q$ , i.e.,  $p = qp_s(q)$ . The steady state occupancies are then given by [28, Eqn. 10.16]

$$\mathbb{E}\tau_i = \frac{(1 - qp_s) \sum_{n=0}^{N-i} B(N-n)B(n) + qp_s B(N)}{B(N+1) + qp_s B(N)}, \quad (23)$$

where  $B(0) = 1$ , and

$$B(k) = \sum_{j=0}^{k-1} \frac{1}{k} \binom{k}{j} \binom{k}{j+1} (1 - qp_s)^j, \quad k > 0.$$

The steady state occupancies depend non-trivially on the product term  $qp_s$ , as depicted in Fig. 9. As in the CSMA-based flow, there exists a particle-hole symmetry,<sup>10</sup> i.e.,

<sup>10</sup> Particles (packets) moving towards the destination are equivalent to holes (empty buffers) moving towards the source.

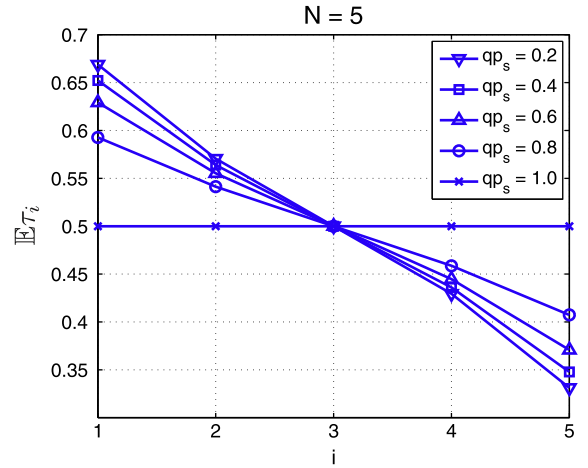


**Fig. 9.** Average node occupancies at steady state for an ALOHA-based flow with  $N=5$  and  $R=1$ . Notice that they depend non-trivially on the product term  $qp_s$ . The particle-hole symmetry holds here as well:  $\mathbb{E}\tau_i = 1 - \mathbb{E}\tau_{N+1-i}$ .

$\mathbb{E}\tau_i \equiv 1 - \mathbb{E}\tau_{N+1-i}$ . Hence, in a system with an odd number of relays, the middle relay has an occupancy of exactly  $1/2$ . Irrespective of  $p$ , the average number of packets in the flow at steady state is  $\sum_{i=0}^N \mathbb{E}\tau_i = 1 + N/2$ . For the special case  $q = p_s = 1$ , the steady state configuration consists of alternating ones and zeros, and  $\mathbb{E}\tau_i = 1/2, \forall i$ .

### 6.2. Packet success probability

We next measure the packet success probability for a typical link in the ALOHA-based network. Recall that the average number of packets (at steady state) in a flow with  $N$  relays is  $1 + N/2$ . With  $\delta$  being the density of source nodes (or flows) and  $q$  the ALOHA contention probability, it follows that the density of interferers for the ALOHA-based network is at most<sup>11</sup>

$$\lambda_i \lesssim \delta q (1 + N/2). \quad (24)$$

Even though transmissions in the network are completely uncoordinated, the interference is actually spatially and temporally correlated owing to the presence of common randomness in the locations of nodes [29]. However, for analytical tractability, we make the relaxed assumption that the set of interfering nodes forms a PPP with density  $\lambda_i$ , which is quite accurate at small  $q$  [29].

We then have the following proposition concerning the packet success probability over a typical link between a node and its  $n$ th-nearest-neighbor in the ALOHA-based network.

**Proposition 6.1.** *For the ALOHA-based flow across  $N$  relays, the packet success probability  $p_s$  from any node to its  $n$ th-nearest-neighbor in a sector of angle  $\phi$  is*

<sup>11</sup> This term is actually an upper bound, owing to the existence of relay nodes having multiple packets in their buffers (corresponding to several flows). The bound is tight for small  $q$  (when the density of interferers is small), or small  $\delta$  (when the flows in the network themselves are sparse).

$$p_s = \left( \frac{(1-\delta)\phi}{(1-\delta)\phi + 2\lambda_1 c} \right)^n. \quad (25)$$

where  $\lambda_1$  is given by (24), and  $c = \pi\Gamma(1+2/\gamma)\Gamma(1-2/\gamma)\Theta^{2/\gamma}$ .

**Proof.** The proof is equivalent to the one for Proposition 5.2 with the density of interferers in this case being  $\lambda_1$  (instead of  $\delta$ , for the CSMA-based network).  $\square$

### 6.3. Steady state throughput and average end-to-end delay

The following theorem quantifies the throughput and mean end-to-end delay across a typical flow in the network in closed-form.

**Theorem 6.2.** For an ALOHA-based line flow along  $N$  relays, the steady state throughput is

$$T(N) = \frac{qB(N)}{B(N+1) + qp_s B(N)}, \quad (26)$$

while the average end-to-end delay is given by

$$D(N) = (1 + N/2)/T. \quad (27)$$

**Proof.** The proof is very similar to the one of Theorem 5.3. Indeed, at any instant of time (in steady state), relay node  $N$ 's buffer has a packet w.p.  $\mathbb{E}\tau_N$ ; furthermore, it transmits w.p.  $q$ , and the transmission succeeds w.p.  $p_s$ . Thus, the throughput is simply given by  $T = qp_s \mathbb{E}\tau_N$ , which is identical to (26). (27) follows from Little's theorem.  $\square$

### 6.4. Throughput density

Putting together (24)–(26), we obtain a bound on the throughput density for the ALOHA-based network as

$$\rho_T(N) \gtrsim \frac{\delta q B(N) \left( \frac{(1-\delta)\phi}{(1-\delta)\phi + 2\delta q (1+N/(2\sqrt{n}))c} \right)^n}{B(N+1) + q B(N) \left( \frac{(1-\delta)\phi}{(1-\delta)\phi + 2\delta q (1+N/(2\sqrt{n}))c} \right)^n}. \quad (28)$$

The above equation helps provide useful insights into network design. For instance, the throughput density-maximizing values of  $\delta$  or  $n$  may be computed numerically using (28).

## 7. Common relays serving multiple flows

Note that in our analyses, we have neglected the occurrence of the event  $E$ , wherein an arbitrarily chosen relay serves multiple routes at the same time. It is important to consider  $E$  in the analysis because if it happens often, the density of interferers would be smaller. Also, the occurrence of  $E$  would mean that the average number of successful packet receptions in any time slot is reduced (assuming that typical  $\Theta$  values are  $>1$ ) since each relay can successfully receive at most one packet (corresponding to the transmitter with the strongest channel to that relay). Moreover, event  $E$  may lead to a

'transmit bottleneck', where relays end up with multiple packets in their buffer and the transmission scheduling algorithms may then get complicated. However, we argue in the following that ignoring the occurrence of  $E$  is not critical and that our analyses are still quite accurate. We also later verify this argument via simulation results in Section 8.

We begin by approximating the arrangement of flows in the network as a *Poisson line segment process* [30], according to which the mid-segment points form a PPP of density  $\delta$ , and take that all the nodes involved in the flows are located on the corresponding line segments. Also, the segments are uniformly randomly oriented, and the lengths of the line segments are finite and random, drawn according to a certain distribution function  $F_L(l)$ . As per [30, Eq. 14], the density of intersecting points,  $\lambda_i$ , is given by  $\lambda_i = (\delta \mathbb{E}L)^2/\pi$ . When  $\delta$  is small, this is already much smaller than unity (which is the total density of the considered network). For instance, taking  $\delta = 0.05$  and  $\mathbb{E}L = 5$  yields  $\lambda_i = 0.02 \ll 1$ . Now, the density of relay nodes serving multiple flows is smaller than  $\lambda_i$ , since the points of intersection of the line segments do not always correspond to common relay nodes' locations. Furthermore, the probability that two nodes corresponding to two intersecting flows transmit to the same (common) relay in the same time slot for either MAC schemes (CSMA or ALOHA) is even smaller – given that a node in the first flow transmits a packet to that (common) relay, the probability that another node (along the second flow) also transmits to it in the same time slot<sup>12</sup> is simply its access probability. Thus, the occurrence of  $E$  is quite rare.

A few ways to circumvent the consideration of  $E$  are as follows. First, we may assume  $\delta \ll 1$ , for which relays serving multiple flows are rare (as we have seen above using ideas from the theory of Poisson line segment processes), and the expression concerning the density of interferers is quite accurate. Second, the MAC scheme may be modified such that relays having multiple packets may schedule them in a sequential fashion. This however leads to an increased end-to-end delay (and a decreased throughput) since packets stay in queues longer. Third, the routing protocol may be revised such that packets are not routed through relays that already support another flow. Modeling the interference (and in turn, the success probabilities) is tricky in this case though, since the set of interferers no longer forms a PPP.

## 8. Simulation results

We now provide simulation results to illustrate the theoretical results. All the results are obtained using MATLAB. The simulated mesh network comprises nodes arranged as a PPP with unit density on a  $50 \times 50$  square. Thus, on average, there exist 2500 nodes in the network. We also choose the following values for the system parameters: the source density  $\delta = 0.01$ , the SIR threshold  $\Theta = 10$  dB, the routing

<sup>12</sup> The probability of  $k \geq 2$  nodes transmitting to that common relay in the same time slot is  $1/N^k$ , and decays fast to 0 with increasing  $k$ .

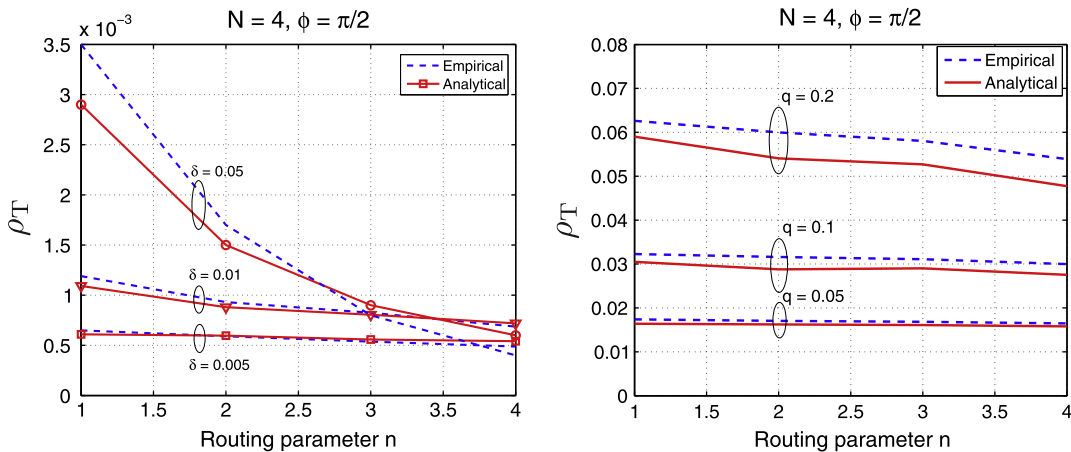


**Fig. 10.** Theoretical and simulation-based plots for  $\rho_T$  versus the routing parameter  $n$  for CSMA-based (left) and ALOHA-based (right) networks. The empirical and analytical values are seen to match closely for a wide range of system parameters, validating our analysis.

angle  $\phi = \pi/2$ , the PLE  $\gamma = 4$ , and the fading to be i.i.d. Rayleigh with unit mean. The throughput of each flow is measured as the rate of packets delivered to the destination, and its steady state value is computed by considering only those packets delivered during the time slots 3000 through 5000. In order to avoid border effects, we collect the metrics only for those routes completely lying in the inner square of dimensions  $40 \times 40$ . We obtain results from 100 different realizations of the point process, which is found to be sufficient to obtain good statistical confidence. Fig. 10 plots the steady state throughput density in both the CSMA- and ALOHA-based for  $N = 4$ . In both cases, we observe that the empirical and analytical values match closely for a wide range of system parameters, thus corroborating the theory.

### 9. Throughput-delay tradeoff

It is interesting to study the achievable tradeoff between the throughput and delay across a typical flow for both the MAC schemes. For the CSMA-based network, we may use (9) and (10) to see that the ratio  $D(N)/T(N)$  is a cubic function of  $N$ .

As expected, the ALOHA-based network obtains a much better tradeoff since it incorporates spatial reuse. Fig. 11 plots the ratio  $D/T$  versus  $N$  (using (26) and (27)) for the ALOHA-based network for some values of the effective link reliability  $p = qp_s$ . It is seen that  $D/T$  is (approximately) a linear function of  $N$ ; this is verified by the dashed lines that are also shown in the figure.

We now show that the ALOHA-based network achieves the same tradeoff scaling that is obtained for the optimal operation of a wireless network flow. To this end, consider a wireless flow across  $N$  relay nodes. It is always possible to choose the *optimal spatial-reuse parameter*  $m$ , which is the minimum number of hops separating any two transmitters  $i$  and  $j$  such that both their transmissions are successful, i.e., at each receiver node, the condition  $\text{SINR} > \theta$  holds. The optimal scheduling scheme thus is to have every  $m$ th

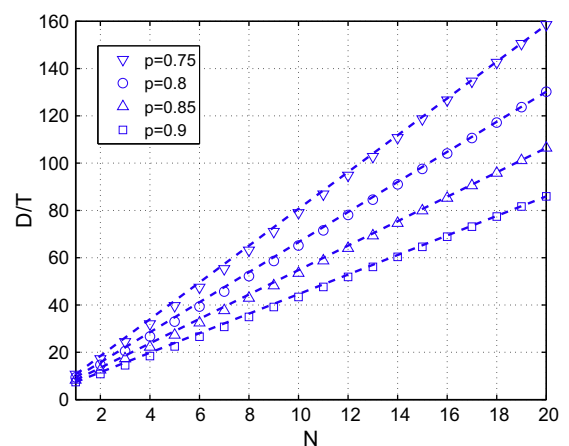


**Fig. 11.** The plot of  $D/T$  versus  $N$  for the ALOHA-based network for some values of the link reliability  $p$ . The (dashed) lines  $D/(NT)$  illustrate that  $D \propto NT$  (approximately).

node transmit simultaneously.<sup>13</sup> Indeed, for this case, all transmissions are successful; the network end-to-end delay is minimal, and equal to  $N + 1$  time slots. Also, the throughput attains its maximum value (of  $1/m$ ). Thus, the optimal throughput-delay scaling for a wireless network flow is obtained as  $D \propto NT$ .

The optimal scheduling that minimizes the end-to-end delay (and maximizes the throughput) in a flow with  $N = 10$  relays is illustrated in Fig. 12, for  $m = 3$ . This MAC scheme can be implemented by simply having all nodes with packets transmit; it can be viewed as ALOHA with transmit probability 1.

In the above scenario, all the transmissions are successful. However, in the presence of fading, unequal spacing between the nodes, or interference from other networks, transmissions can fail, and the ALOHA scheme with contention parameter 1 may perform sub-optimally. Nevertheless,

<sup>13</sup> A centralized scheduler is, however, required to perform this operation.

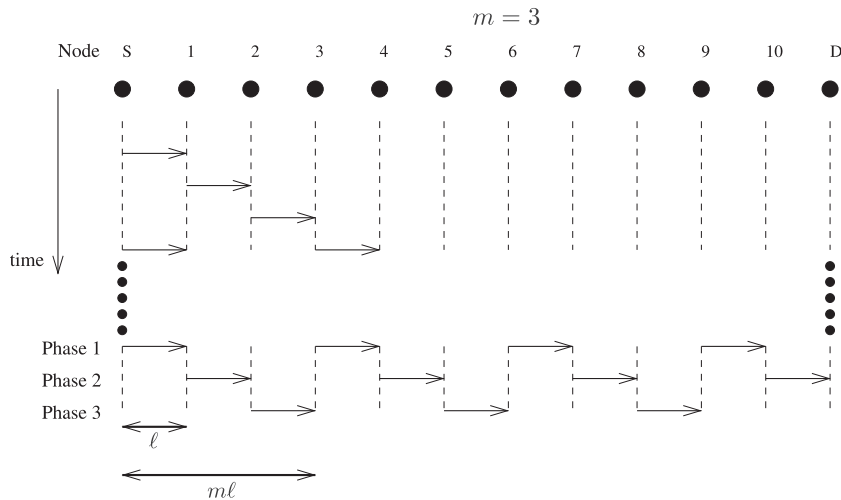


**Fig. 12.** The optimal scheduling assignment (in the absence of fading) for a multihop flow with 10 relay nodes for  $m = 3$ . Here,  $\ell$  is the spacing between adjacent relays. In the steady state (long-time limit), there are three unique transmission phases, in each of which nodes three hops apart transmit simultaneously. The system achieves a throughput of  $1/3$  and an end-to-end delay of 11 time slots for each packet.

this example illustrates that for efficient network operation, it is necessary that the transmitting nodes not be too closely located. In fact, for half-duplex nodes,  $m$  needs to be always kept  $\geq 2$ . Also, since adjacent nodes cannot both transmit successfully at the same time, it is not necessary to have  $K > 1$  as packets are never stacked; unit-sized buffers ( $K = 1$ ) are sufficient for optimal network operation.

## 10. Summary

We consider a planar Poisson network comprising infinite packet flows from several sources to several destinations. Using concepts and tools from both stochastic geometry and statistical mechanics, in particular, the TASEP particle flow model, we analytically characterize the system throughput for two different channel access schemes. We also provide valuable insights from a network design stand-point such as choosing the optimum density of transmitters and the number of hops in each route in the network such that the spatial throughput density is maximized. We wish to promote the TASEP as a powerful tool for the study and design of mesh networks.

We would also like to remark that we use the same (constant) number of hops  $N$  in each flow for analytical tractability, in particular to obtain closed-form expressions for the optimal network design parameters  $n_{\text{opt}}$  and  $\delta_{\text{opt}}$ . The results in this paper may however be generalized to the case wherein the lengths of the flows are different. Indeed, we may simply treat  $N$  to be a random variable with a certain distribution or a flow-specific value (that way, all destinations are at random distances from their corresponding sources); the throughput density would then simply have to be averaged w.r.t. the distribution of  $N$ .

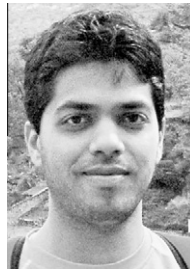
## Acknowledgments

This work has been supported by the NSF (Grants CNS 04-47869, CCF 728763) and the DARPA/IPTO IT-MANET program (grant W911NF-07-1-0028).

## References

- [1] J. Andrews, N. Jindal, M. Haenggi, R. Berry, D. Guo, M. Neely, S. Weber, S. Jafar, A. Yener, Rethinking information theory for mobile ad hoc networks, *IEEE Communications Magazine* 46 (2008) 94–101.
- [2] A. Goldsmith, S.B. Wicker, Design challenges for energy-constrained ad hoc wireless networks, *IEEE Wireless Communications Magazine* 9 (4) (2002) 8–27.
- [3] R.C. Alamino, D. Saad, Statistical mechanics analysis of LDPC coding in MIMO Gaussian channels, *Journal of Physics A: Mathematical and Theoretical* 40 (41) (2007) 12259–12279.
- [4] K. Takeuchi, T. Tanaka, Statistical-mechanics-based analysis of multiuser MIMO channels with linear dispersion codes, *Journal of Physics: Conference Series* 95 (1) (2008).
- [5] D. Guo, S. Verdú, Randomly spread CDMA: asymptotics via statistical physics, *IEEE Transactions on Information Theory* 51 (2005) 1261–1282.
- [6] M.B. Hastings, Statistical mechanics of interfering links, *Physics Review E* (2005).
- [7] K.H. Hui, D. Guo, R. Berry, M. Haenggi, “Performance analysis of MAC protocols in wireless line networks using statistical mechanics,” in: *Proceedings of the 47<sup>th</sup> annual Allerton Conference on Communication, Control, and Computing*, IEEE press Piscataway, NJ, USA, September 2009.
- [8] M. Franceschetti, R. Meester, *Random Networks for Communication: From Statistical Physics to Information Systems*, Cambridge University Press, 2008.
- [9] M. Haenggi, J.G. Andrews, F. Baccelli, O. Dousse, M. Franceschetti, Stochastic geometry and random graphs for the analysis and design of wireless networks, *IEEE Journal on Selected Areas in Communications* 27 (7) (2009) 1029–1046.
- [10] N. Rajewsky, L. Santen, A. Schadschneider, M. Schreckenberg, The asymmetric exclusion process: comparison of update procedures, *Journal of Statistical Physics* 92 (1/2) (1998) 151–194.
- [11] S. Xu, T. Saadawi, Does the IEEE 802.11 MAC protocol work well in multihop wireless adhoc networks?, *IEEE Communications Magazine* 36 (6) (2001) 130–137.
- [12] Z. Fu, P. Zerfos, H. Luo, S. Lu, L. Zhang, M. Gerla, The impact of multihop wireless channel on TCP throughput and loss, *INFOCOM 2003* 3 (2003) 1744–1753.
- [13] J. Li, C. Blake, D.S.J. De Couto, H.I. Lee, R. Morris, Capacity of ad hoc wireless networks, in: *Proc. ACM International Conference on Mobile Computing and Networking*, July 2001, pp. 61–69.
- [14] V. Gupta, On the effect of transmission delay on estimation, *IEEE Transactions on Automatic Control* (accepted for publication).
- [15] L. Tassiulas, Adaptive back-pressure congestion control based on local information, *IEEE Transactions on Automatic Control* 40 (2) (1995) 236–250.

- [16] M. Haenggi, On routing in random Rayleigh fading networks, *IEEE Transactions on Wireless Communications* 4 (4) (2005) 1553–1562.
- [17] E.S. Sousa, J.A. Silvester, Optimum transmission ranges in a direct-sequence spread-spectrum multi-hop packet radio network, *IEEE Journal on Selected Areas in Communications* 8 (1990) 762–771.
- [18] F. Baccelli, B. Błaszczyszyn, P. Mühlenthaler, An Aloha protocol for multihop mobile wireless networks, *IEEE Transactions on Information Theory* 52 (2) (2006) 421–436.
- [19] F. Baccelli, B. Błaszczyszyn, P. Mühlenthaler, Stochastic analysis of spatial and opportunistic Aloha, *IEEE Journal on Selected Areas in Communications* 27 (7) (2009) 1105–1119.
- [20] S.P. Weber, J.G. Andrews, X. Yang, G. de Veciana, Transmission capacity of wireless ad hoc networks with successive interference cancellation, *IEEE Transactions on Information Theory* 53 (8) (2007) 2799–2814.
- [21] K. Stamatiou, F. Rossetto, M. Haenggi, T. Javidi, J.R. Zeidler, M. Zorzi, A delay-minimizing routing strategy for wireless multihop networks, in: *Fifth Workshop on Spatial Stochastic Models for Wireless Networks (SpaSWIN)*, June 2009.
- [22] K. Stamatiou, M. Haenggi, The delay-optimal number of hops in Poisson multi-hop networks, in: *IEEE Symposium of Information Theory (ISIT)*, June 2010.
- [23] K. Stamatiou, M. Haenggi, Optimal spatial reuse in Poisson multi-hop networks, in: *IEEE Global Communications Conference (GLOBECOM)*, December 2010.
- [24] M. Haenggi, On distances in uniformly random networks, *IEEE Transactions on Information Theory* 51 (2005) 3584–3586.
- [25] B. Derrida, E. Domany, D. Mukamel, An exact solution of a one-dimensional asymmetric exclusion model with open boundaries, *Journal of Statistical Physics* 69 (3/4) (1992) 667–687.
- [26] L. Kleinrock, *Queueing Systems, Theory*, vol. I, Wiley, 1975.
- [27] M. Haenggi, D. Puccinelli, Routing in ad hoc networks: a case for long hops, *IEEE Communications Magazine* 43 (2005) 93–101.
- [28] M.R. Evans, N. Rajewsky, E.R. Speer, Exact solution of a cellular automaton for traffic, *Journal of Statistical Physics* 95 (1/2) (1999).
- [29] R.K. Ganti, M. Haenggi, Spatial and temporal correlation of the interference in ALOHA ad hoc networks, *IEEE Communication Letters* 13 (9) (2009) 631–633.
- [30] P. Parker, R. Cowan, Some properties of line segment processes, *Journal of Applied Probability* 13 (1) (1976) 96–107.



**Sunil Srinivasa** (S'06) is a Ph.D. candidate in the department of Electrical Engineering at the University of Notre Dame, Indiana, USA. He received the B. Tech degree in electrical engineering from the Indian Institute of Technology, Madras (IITM) in 2004 and the M.S. degree in electrical engineering from the University of Notre Dame in 2007. His research interests include wireless communications and networking and information theory.



**Martin Haenggi** (S'95, M'99, SM'04) is an Associate Professor of Electrical Engineering and a Concurrent Associate Professor of Applied and Computational Mathematics and Statistics at the University of Notre Dame, Indiana, USA. He received the Dipl. Ing. (M.Sc.) and Ph.D. degrees in electrical engineering from the Swiss Federal Institute of Technology in Zurich (ETHZ) in 1995 and 1999, respectively. After a postdoctoral year at the Electronics Research Laboratory at the University of California in Berkeley, he joined the faculty of the electrical engineering department at the University of Notre Dame in 2001. In 2007–2008, he spent a Sabbatical Year at the University of California at San Diego (UCSD). For both his M.Sc. and his Ph.D. theses, he was awarded the ETH medal, and he received a CAREER award from the US ~ National Science Foundation in 2005 and the 2010 IEEE Communications Society Best Tutorial Paper award. He served as a member of the Editorial Board of the Elsevier Journal of Ad Hoc Networks from 2005–2008 and as a Distinguished Lecturer for the IEEE Circuits and Systems Society in 2005–2006. Presently he is an Associate Editor the IEEE Transactions on Mobile Computing and the ACM Transactions on Sensor Networks. His scientific interests include networking and wireless communications, with an emphasis on ad hoc, cognitive, mesh, and sensor networks.